Eur. Phys. J. Plus (2016) **131**: 89
DOI 10.1140/epjp/i2016-16089-3

THE EUROPEAN PHYSICAL JOURNAL PLUS

Regular Article

Effect of annealing temperature on morphological, structural and optical properties of nanostructured CuO thin film

Unal Akgul[a], Koksal Yildiz[b], and Yusuf Atici[c]

Department of Physics, Faculty of Science, Firat University, 23119 Elazig, Turkey

Received: 14 December 2015
Published online: 12 April 2016 –

Abstract. CuO thin film was grown on a glass substrate by reactive radio frequency (rf) magnetron sputtering. The deposited film was annealed in air at various temperatures for 2 h. The SEM images showed that the grain size increased with rising annealing temperature. The EDX and XRD results revealed that the chemical composition and phase of the polycrystalline film were not affected by the annealing conditions. The optical band gap increased from 2.244 eV to 2.261 eV and then decreased from 2.261 eV to 2.145 eV by the effect of annealing temperature.

1 Introduction

CuO (cupric oxide, tenorite) is a very useful material for many applications such as transistors, light-emitting diodes, electrochromic devices, lithium ion batteries, high-temperature superconductors, gas sensors and solar cells [1,2]. Especially, CuO thin film has become a promising material for solar energy system because of its suitable optical band gap of 1.3–2.1 eV [3,4]. Therefore, the effect of annealing temperature on the structural and optical properties of CuO thin film was investigated by many researchers. Thermal annealing is a widely used method to improve crystal quality and to study structural defects in materials [5]. The type and amount of defect are dependent on the annealing temperature and atmosphere [6]. Also, these annealing conditions can change the crystal phase of the film. Murali *et al.* have reported that the annealing of CuO thin films in vacuum at 623 K and 700 K results in the formation of a new phase in the structure of the films [7]. In most studies, the low annealing temperatures were used.

In this study, CuO thin film was deposited using reactive rf magnetron sputtering technique and then annealed in air at different temperatures up to 600 °C. The morphological, structural and optical properties of the unannealed and annealed films were investigated.

2 Experimental

2.1 Sample preparation

CuO thin film was prepared using a NANOVAK combined system. Prior to the deposition process, the glass substrate ($20 \times 20\,mm^2$) was ultrasonically cleaned in acetone and methanol for 10 min to remove the contamination such as dusts, spots, oils, fingerprints, etc. The dried substrate was mounted on a temperature-controlled and rotating substrate holder in the deposition chamber. The chamber was evacuated to a base pressure of $3 \cdot 10^{-8}$ Torr. In order to remove the oxide layer on the target surface, the copper target (with purity of 99.999%) was bombarded with argon ions for 10 min prior to the deposition. After presputtering, CuO thin film with a thickness of 200 nm was grown at a total gas pressure of 10 mTorr (77% Ar + 23% O_2) on the glass substrate. During the sputter deposition, the rf power and substrate temperature were fixed at 75 W and 200 °C, respectively. The flow rates for argon and oxygen were 4.0 and 1.2 sccm, respectively. The deposition rate was ~ 0.75 Å/s. The deposited film was annealed in air at 200, 400 and 600 °C for 2 h. The unannealed film was termed F1, while the films annealed at 200, 400 and 600 °C were termed F2, F3 and F4, respectively.

[a] e-mail: uakgul@firat.edu.tr (corresponding author)
[b] e-mail: kyildiz@firat.edu.tr
[c] e-mail: yatici@firat.edu.tr

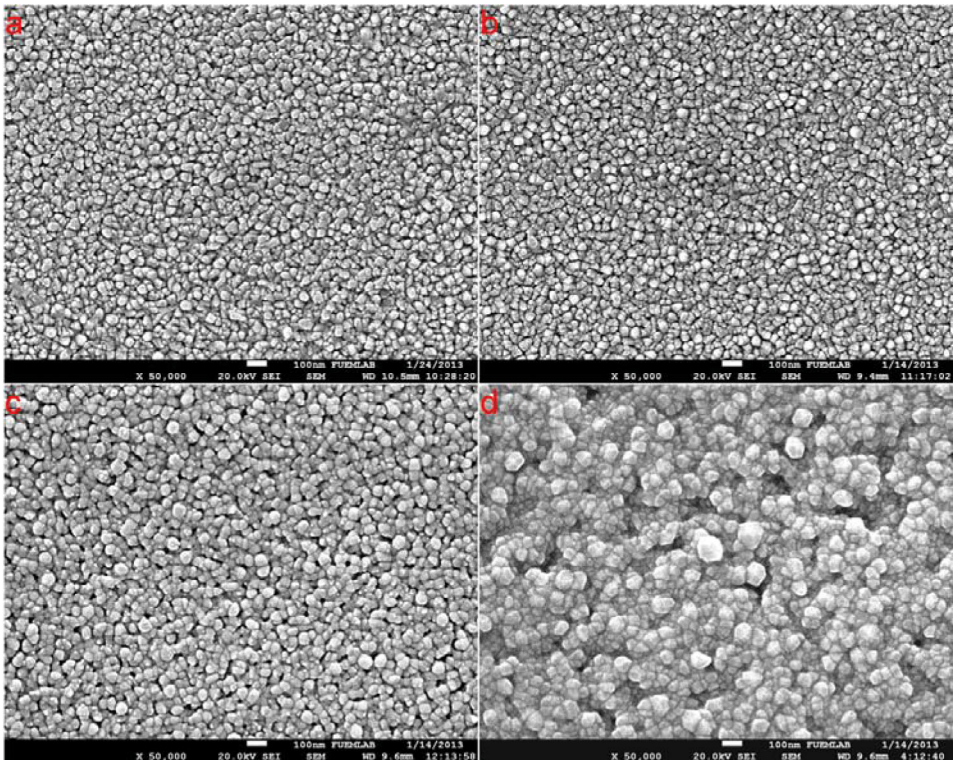

Fig. 1. SEM images of the thin films (a. F1, b. F2, c. F3, d. F4).

2.2 Measurements

The films were coated with gold for the surface morphology observations. The surface morphologies of the films were analyzed by a JEOL JSM-7001F scanning electron microscopy (SEM). The chemical compositions were identified by using an OXFORD INCA energy dispersive X-ray (EDX) detector. The EDX studies were done at accelerating voltage of 6 kV. X-ray diffraction (XRD) analyses for phase identification were performed using a RIGAKU SmartLab X-ray diffractometer. CuKα_1 radiation with a wavelength of 1.544 Å was used for XRD analyses. The optical properties were characterized by a Perkin Elmer Precisely Lambda 45 UV/VIS Spectrometer.

3 Results and discussion

3.1 Structural properties

Figure 1 shows the SEM images of the films at ×50000 magnification. The surface morphologies of the films consist of the randomly oriented grains and voids among the grains. Such a surface structure of the unannealed thin film is consistent with the results expected by Thornton's structure-zone model. The films have a dense and crack-free surface morphology. The grain size in F1, F2, F3 and F4 films varied in the ranges of approximately 7–67, 7–69, 9–76 and 24–151 nm, respectively. Additionally, no significant difference was observed between the morphologies of F1 and F2 films. This observation indicates that the recrystallization temperature is higher than the annealing temperature of 200 °C [8]. However, the residual stress in F2 film may be greatly reduced. At higher annealing temperatures, new grains appear and grow by the influence of recrystallization as shown in figs. 1c and 1d. The resulting strain-free grains replace the old strained grains [9]. While the grains in F3 film tend to take on a spherical shape, the grains in F4 film have a polyhedral shape. In addition, the grain boundaries in the coarse-grained F4 film began to be uncertain. This finding signifies the deterioration in surface morphology.

Figure 2 illustrates the EDX spectra of the thin films. From the spectral data given in table 1, it can be seen that all of the films have the same chemical composition. The carbon peak at around 0.277 keV is caused by the charge-up on the surface of the films during EDX analyses.

The XRD patterns of the films are given in fig. 3. The diffraction peaks were indexed according to JCPDS card numbered 01-080-0076 ($a = 4.6797$ Å, $b = 3.4314$ Å, $c = 5.1362$ Å, $\beta = 99.262°$). The XRD analyses displayed that the films were polycrystalline. The polycrystalline films exhibited well crystallization on the $(\bar{1}11)$ reflection plane. The low-intensity diffraction peaks are evident at high annealing temperatures. The sharp and intense peaks demonstrate better and enhanced crystallinity [10–13]. XRD patterns did not reveal the presence of a second phase or

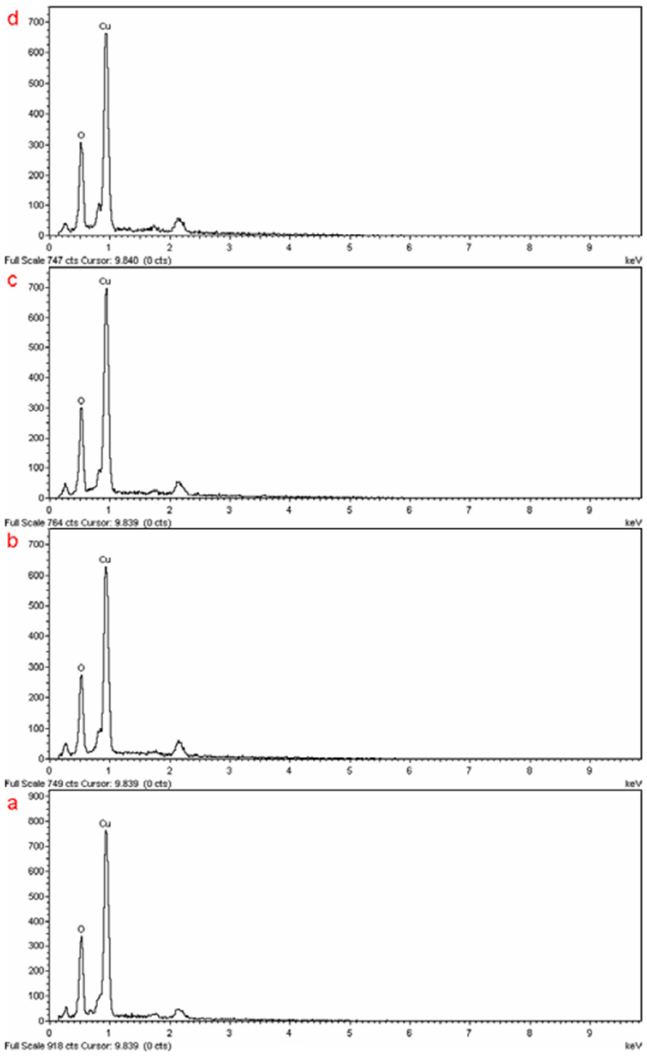

Fig. 2. EDX spectra of the thin films (a. F1, b. F2, c. F3, d. F4).

Table 1. The results of EDX analyses.

Film	Element	Weight %	Atomic %
F1	Cu	79.82	49.90
	O	20.18	50.10
F2	Cu	80.75	51.37
	O	19.25	48.63
F3	Cu	80.83	51.50
	O	19.17	48.50
F4	Cu	79.49	49.40
	O	20.51	50.60

impurities. The CuO phase remained unchanged after annealing. This similarity between the EDX and XRD results is related to the annealing environment. When the annealing treatment is carried out in air, atmospheric oxygen can be adsorbed at the surface of the films and the grain boundary to form negatively charged oxygen species [6]. Thus, the CuO phase remains the same. With raising annealing temperature, the $(\bar{1}11)$ diffraction peak was slightly shifted to high 2θ angles due to the residual stress [14]. Large residual stresses are commonly found in sputtered thin films [15].

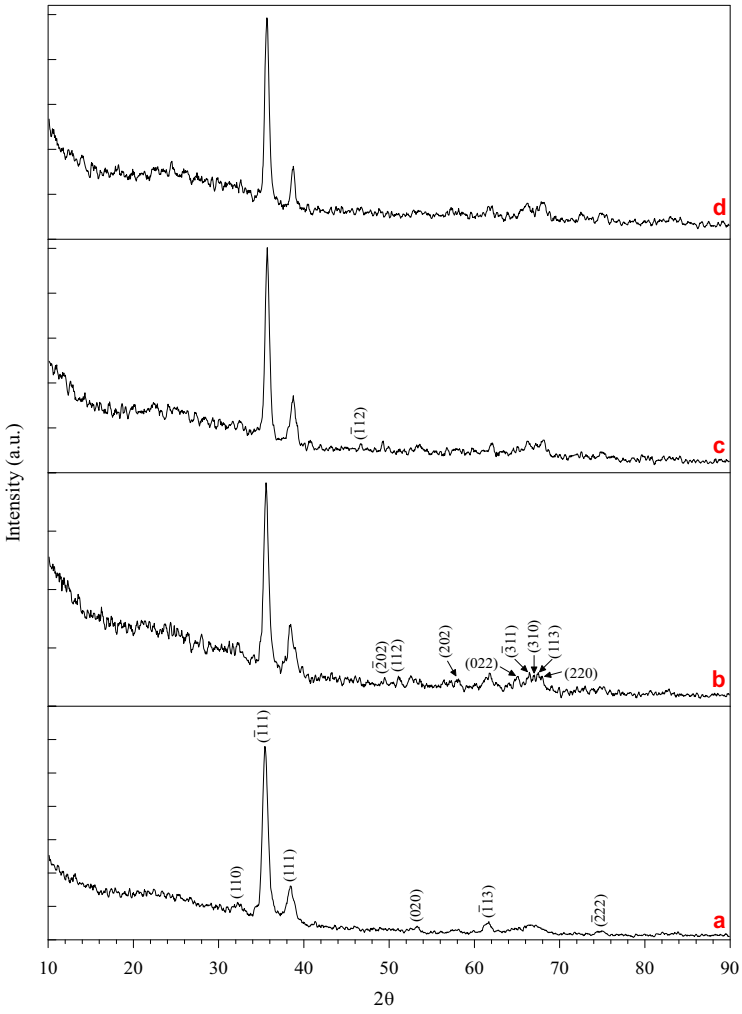

Fig. 3. XRD patterns of the thin films (a. F1, b. F2, c. F3, d. F4).

3.2 Optical properties

Figure 4 presents the variation of transmittance with wavelength for all the films. The films exhibited the highest transmittance in the near-infrared region. The highest transmittance values for F1, F2, F3 and F4 films were 73.11%, 79.14%, 79.19% and 70.12%, respectively. A similar rise in transmittance was interpreted as the reduction of unsaturated bonds by Zhao *et al.* [16]. However, the grain coarsening at higher temperatures contributes to the decrease in film transparency. The phase of the film also plays a major role in the change of transmittance values. The CuO crystal is biaxial and optically anisotropic due to its monoclinic crystal structure. Therefore, it leads to the double refraction. The double refraction in a polycrystalline film causes light scattering [17,18]. The location of the transmission peak varied up to 845 nm with the increment of temperature. Such a result is related to the shift of the absorption edge toward higher wavelength and lower energy. In the literature, this is called the red shift.

It is well known that the increase in the grain size could cause the red shift [19].

The relationship between the absorption coefficient (α) and the photon energy ($h\nu$) is expressed as

$$\alpha h\nu = A(h\nu - E_{\mathrm{g}})^{\mathrm{n}},$$

where A is a constant, E_{g} is the optical band gap energy and n is an exponent that depends on the type of transition. The value of n is 1/2, 2, 3/2 and 3 corresponding to allowed direct, allowed indirect, forbidden direct and forbidden indirect transition, respectively [20–22]. In order to determine the optical band gap value (E_{g}) of the thin films, the graph of $(\alpha h\nu)^2$ *versus* $h\nu$ was plotted (fig. 5). The band gaps of F1, F2, F3 and F4 thin films were found to be 2.244, 2.261, 2.153 and 2.145 eV, respectively. The sudden rise in the optical band gap can be associated with the elimination of residual stress in the film structure. The variation of E_{g} with annealing temperature is demonstrated in the inset of fig. 5. With the grain size increment, the absorption edge shifted from 550 nm to about 575 nm. This change gave rise to the narrowing of the band gap.

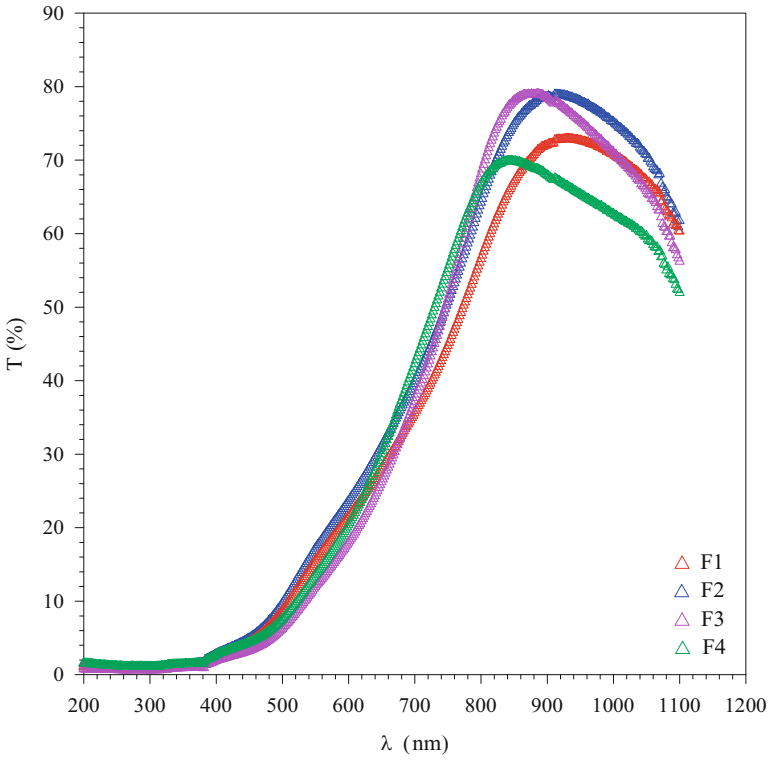

Fig. 4. Variation of transmittance with wavelength.

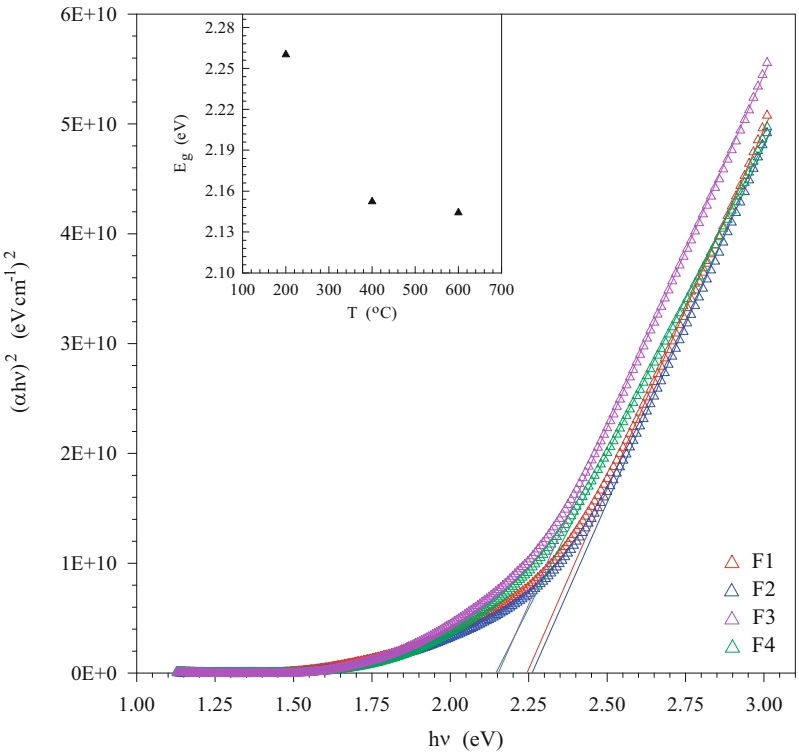

Fig. 5. Dependence of $(\alpha h\nu)^2$ on the photon energy. (The inset demonstrates the annealing temperature dependence of the optical band gap.)

4 Conclusion

The single-phase CuO thin film was successfully grown by reactive rf magnetron sputtering under the total gas pressure of 10 mTorr (77% Ar + 23% O_2). The higher annealing temperatures were used in this study. When the temperature was increased, the grain coarsening occurred. The unannealed and annealed films have a high absorbance of light in the visible and near-infrared regions. The optical band gap of the film decreased from 2.261 eV to 2.145 eV with the increase of the annealing temperature from 200 °C to 600 °C. The obtained band gap values are close to the values recorded in the literature. The differences in values were attributed to the sputtering parameters and annealing conditions. The crystal phase and chemical composition of the film did not change by the effect of annealing. It was predicted that the structure of CuO thin film deteriorated at temperatures higher than 600 °C. The annealing atmosphere is an important factor for changes in the chemical properties of the film. These results support several conclusions.

This study was supported by the Management Unit of Scientific Research Projects of Firat University (Project no: 1386). We thank BioNanoTechnology Research and Development Center of Fatih University for the XRD analyses.

References

1. B. Pecquenard, F. Le Cras, D. Poinot, O. Sicardy, J-P. Manaud, ACS Appl. Mater. Interf. **6**, 3413 (2014) DOI: 10.1021/am4055386.
2. T. Shrividhya, G. Ravi, Y. Hayakawa, T. Mahalingam, J. Mater. Sci: Mater. Electron. **25**, 3885 (2014) DOI: 10.1007/s10854-014-2103-z.
3. V. Saravanan, P. Shankar, G.K. Mani, J.B.B. Rayappan, J. Anal. Appl. Pyrol. **111**, 272 (2015) DOI: 10.1016/j.jaap.2014.08.008.
4. R. Shabu, A.M.E. Raj, C. Sanjeeviraja, C. Ravidhas, Mater. Res. Bull. **68**, 1 (2015) DOI: 10.1016/j.materresbull.2015.03.016.
5. J. Yang, M. Gao, Y. Zhang, L. Yang, J. Lang, D. Wang, H. Liu, Y. Liu, Y. Wang, H. Fan, Superlattice. Microst. **44**, 137 (2008) DOI: 10.1016/j.spmi.2008.04.006.
6. B.L. Zhu, X.Z. Zhao, F.H. Su, G.H. Li, X.G. Wu, J. Wu, R. Wu, Vacuum **84**, 1280 (2010) DOI: 10.1016/j.vacuum.2010.01.059.
7. D.S. Murali, S. Kumar, R.J. Choudhary, A.D. Wadikar, M.K. Jain, A. Subrahmanyam, AIP Adv. **5**, 047143, 1 (2015) DOI: 10.1063/1.4919323.
8. U. Akgul, PhD Thesis, Firat University, Turkey (2015).
9. H.L. Walker, *Grain sizes produced by recrystallization and coalescence in cold-rolled cartridge brass* (University of Illinois, Urbana, 2007).
10. S. Mahato, A.K. Kar, J. Electroanal. Chem. **742**, 23 (2015) DOI: 10.1016/j.jelechem.2015.01.034.
11. S. Chander, M.S. Dhaka, Physica E **73**, 35 (2015) DOI: 10.1016/j.physe.2015.05.008.
12. M. Kawwam, F.H. Alharbi, T. Kayed, A. Aldwayyan, A. Alyamani, N. Tabet, K. Lebbou, Appl. Surf. Sci. **276**, 7 (2013) DOI: 10.1016/j.apsusc.2013.02.051.
13. B.S. Soram, B.S. Ngangom, H.B. Sharma, Thin Solid Films **524**, 57 (2012) DOI: 10.1016/j.tsf.2012.09.015.
14. N. Rahmani, R.S. Dariani, Superlattice. Microst. **85**, 504 (2015) DOI: 10.1016/j.spmi.2015.05.048.
15. R. Hong, J. Huang, H. He, Z. Fan, J. Shao, Appl. Surf. Sci. **242**, 346 (2005) DOI: 10.1016/j.apsusc.2004.08.037.
16. B. Zhao, J. Zhou, Y. Chen, Y. Peng, J. Alloy. Compd. **509**, 4060 (2011) DOI: 10.1016/j.jallcom.2011.01.020.
17. T. Maruyama, Sol. Energ. Mat. Sol. C. **56**, 85 (1998) DOI: 10.1016/S0927-0248(98)00128-7.
18. S. Kose, F. Atay, V. Bilgin, I. Akyuz, Mater. Chem. Phys. **111**, 351 (2008) DOI: 10.1016/j.matchemphys.2008.04.025.
19. J.Y. Park, T.H. Kwon, S.W. Koh, Y.C. Kang, B. Kor. Chem. Soc. **32**, 1331 (2011) DOI: 10.5012/bkcs.2011.32.4.1331.
20. S. Visalakshi, R. Kannan, S. Valanarasu, H-S. Kim, A. Kathalingam, R. Chandramohan, Appl. Phys. A **120**, 1105 (2015) DOI: 10.1007/s00339-015-9285-y.
21. H-C. Lu, C-L. Chu, C-Y. Lai, Y-H. Wang, Thin Solid Films **517**, 4408 (2009) DOI: 10.1016/j.tsf.2009.02.079.
22. B. Saha, R. Thapa, K.K. Chattopadhyay, Sol. Energ. Mat. Sol. C. **92**, 1077 (2008) DOI: 10.1016/j.solmat.2008.03.024.